Dispersion of Single-Walled Carbon Nanotubes with an Extended Diazapentacene Derivative†

Aurelio Mateo-Alonso,*,‡ Christian Ehli,§ Kok Hao Chen,§ Dirk M. Guldi,*,§ and Maurizio Prato*,‡

Center of Excellence for Nanostructured Materials (CENMAT), Dipartimento di Scienze Farmaceutiche, INSTM UdR di Trieste, Università di Trieste, Piazzale Europa 1, 34127 Trieste, Italy, and Department of Chemistry and Pharmacy, Interdisciplinary Center for Molecular Materials (ICMM), Friedrich-Alexander-Universität Erlangen-Nürnberg, Egerlandstr. 3, 91058 Erlangen, Germany

Received: August 15, 2007; In Final Form: September 25, 2007

The dispersion of SWCNTs by using a novel diazapentacene derivative is reported. The proposed $\pi-\pi$ interactions between the diazapentacene derivative and SWCNTs leave their inherent properties virtually intact, as observed by several photophysical measurements. This approach is very attractive for manipulation of SWCNTs for electronic applications.

Introduction

Organic derivatives composed of fused aromatic rings such as acenes[1] and carbon nanotubes[2,3] are among the most promising candidates as organic semiconductors for the preparation of electronic devices.[4] The investigation toward the implementation of acenes in electronic devices is facilitated by the fact that they can be synthesized, purified, characterized, and handled through standard organic chemistry procedures. However, single wall carbon nanotubes (SWCNTs) behave similarly to polymers;[5] most often they do not exist individually, but form bundles, which are difficult to characterize and process due to their low solubility in organic or aqueous solvents. Even though SWCNTs present enhanced electronic and mechanical properties in comparison to acenes, their implementation in semiconducting devices is more difficult due to handling problems. This problem has been partially solved by functionalization.[5] Covalent functionalization has given excellent results in terms of solubility.[5] However, such functionalization interferes directly with the electronic properties of the tubes by breaking their extended conjugation. On the other hand, supramolecular functionalization can be achieved by using derivatives of anthracene,[6−11] phenanthrene,[12,13] pyrene,[12,14−26] tetracene,[13] pentacene,[13] fullerene,[11] and conjugated polymers.[27−29] These aromatic derivatives interact with the surface of SWCNTs through a combination of $\pi-\pi$ interactions and solvophobic forces, exfoliating partially the bundles and/or bringing individual tubes into solution. An advantage of supramolecular functionalization[5] is that it interferes slightly with the properties of SWCNTs, and thus it can be considered as the best strategy for exploiting their inherent electronic properties. Overall pyrenes have been widely used because pyrene derivatives with a large variety of functional groups can be easily prepared allowing not only the dispersion of SWCNTs but also the formation of hybrids with fullerene,[23] porphyrins,[21,22] nanoparticles,[15,20] polymers,[16,17,19] and proteins.[14,26]

Ideally, for electronic applications, it will be desirable to disperse and manipulate SWCNTs with molecules more suitable for this purpose that can complement or enhance the inherent properties of nanotubes and also that do not disturb the inherent properties of SWCNTs. In this regard, linear acenes and azaacenes have demonstrated a big potential as organic semiconductors.[1] For this purpose, we have prepared a novel diazapentacene derivative, which has a structure analogous to that of pentacene, but fused to a pyrene unit to increase its π-contact. As a matter of fact, SWCNTs were easily dispersed in the presence of diazapentacene **1** by mild sonication (Scheme 1). More importantly, the properties of the SWCNTs were left virtually unaffected and retained, as observed by a wide variety of steady-state and time-dependent photophysical measurements. Only small red shifts on the absorption properties of the nanotubes were observed, while fluorescence (stady state and time dependent) and transient absorption measurements showed no significant variations between SWCNTs and SWCNT/**1** dispersions. Such a low level of disruption makes this approach very attractive for the manipulation and processing of SWCNTs for electronic applications.

Experimental Methods

Instrumentation. NMR spectra were recorded on a Varian (200 MHz) at room temperature. Chemical shifts reported in ppm are referred to tetramethylsilane (TMS). The proton assignments correspond to the lettering in Scheme 1. Mass spectrometry experiments were recorded at Università degli Studi di Trieste on a Perkin Elmer API1 at 5600 eV (electrospray). Atomic force microscopy (AFM) measurements were carried out on a Digital Instruments (Veeco) Nanoscope IIIa using Veeco RTESP7 Tips from samples deposited by spin coating (3000 rpm × 3 min) on silicon wafer. Commercially available products were used without further purification. HiPCO SWCNTs were purchased from CNI, batch CM26-0023-(B), and used as received. The samples were sonicated in a Bransonic 2510 at room temperature (method A) or in a Bransonic 52 modified with a thermostat (method B). Absorption spectra were measured on a Perkin-Elmer UV/vis spectrometer Lambda 2 or a Varian UV−vis−NIR spec-

† Part of the "Giacinto Scoles Festschrift".

* Corresponding authors. E-mail: amateo@units.it (A.M.-A.); dirk.guldi@chemie.uni-erlangen.de (D.M.G.); prato@units.it (M.P.).

‡ Università di Trieste.

§ Friedrich-Alexander-Universität Erlangen-Nürnberg.

10.1021/jp0765648 CCC: $37.00
Published on Web 11/15/2007

trometer Cary 5000. Steady-state emission spectra were recorded on a FluoroMax 3 fluorometer (HORIBA). The measurements were carried out at room temperature. Fluorescence lifetimes were measured with a Fluorolog TCSPC system (HORIBA). The sample was excited by a NanoLED-405 LH (peak wavelength 403 nm), and the signal was detected by a Hamamatsu MCP photomultiplier (type R3809U-50). Femtosecond transient absorption studies were performed with 418 nm laser pulses (1 kHz, 150 fs pulse width) from an amplified Ti:Sapphire laser system (Clark-MXR, Inc.), the laser energy was 200 nJ. UV−vis spectroelectrochemical experiments were performed with a home-built cell and a three-electrode setup: a light-transparent platinum gauze as working electrode, a platinum wire as counter electrode, and a silver wire as quasi reference electrode. Potentials were applied and monitored with a HEKA elektronik potentiostat (type PG 284). The spectra were recorded with a Perkin-Elmer spectrometer Lambda 2.

Synthesis of Diazapentacene 1. Diazapentacene **1** was prepared by condensing pyrenediketone[30] (50 mg, 0.21 mmol) and 2,3-diaminoanthracene (33 mg, 0.21 mmol) in refluxing pyridine (anhydrous, degassed, 5 mL) for 3 days under argon atmosphere. The solvent was evaporated under vacuum, and the residue was taken up with chloroform (300 mL) and washed with HCl (aqueous 1 M, ×3), $NaHCO_3$ (saturated aqueous solution, ×3), and brine (×3). The organic phase was dried over $MgSO_4$, and the solvent was evaporated under vacuum. Diazapentacene **1** was purified by flash chromatography in chloroform as a bright yellow solid (24 mg, 32%).

^{1}H NMR: 9.63 (d, 2H, J = 7.54 Hz, H_A); 8.99 (s, 2H, H_B); 8.30 (d, 2H, J = 7.81 Hz, H_C); 8.23 (dd, 2H, J = 3.17 and 6.00 Hz, H_D); 8.10 (t, 2H, J = 7.71 Hz, H_E); 8.05 (s, 2H, H_F); 7.61 (dd, 2H, J = 3.50 and 6.51 Hz, H_G). MS (ES, CH_3CN, m/z): found 355.1 (M^+ + H), $C_{26}H_{14}N_2$ requires 354.1. IR (NaCl): 3046, 1421, 1357, 1315, 1294, 1089, 1059, 967, 947, 924, 895, 736, 716. UV−vis (THF): 234, 247, 265, 278, 302, 315, 331, 347, 416, 441, 468.

Preparation of SWCNT/1 Dispersions. *Method A.* HiPCO SWCNTs (spatula tip ~0.1 mg) were sonicated in THF (8 mL) in the presence of **1** (1 mg) for 30 min. The solution was centrifuged at 3000 rpm for 10 min, and the gray supernatant was transferred to another centrifuge tube and centrifuged at 5000 rpm for 90 min. The supernatant with the excess of the diazapentacene **1** was discarded, and the deposited nanotubes were resuspended in fresh THF (8 mL).

Method B. HiPCO SWCNTs (spatula tip ~0.1 mg) were stirred vigorously overnight in the presence of **1** (1 mg) in THF (8 mL). The sample was then sonicated (112 W) for 30 min at 20 °C. The resulting suspension of SWCNT/**1** was centrifuged at 6000 rpm for 20 min, and the supernatant was removed. The nanotubes were resuspended in THF (8 mL). A drop of this suspension was then added to THF (3 mL) and sonicated until the nanotubes dispersed. This process was repeated until a stable gray dispersion was obtained.

Results and Discussion

Diazapentacene **1** was prepared in two steps (Scheme 1). First, pyrene was oxidized to the corresponding pyrenediketone,[30] which was subsequently condensed with 2,3-diaminoanthracene yielding **1**. The compound displays a low solubility in organic solvents, which did not allow the acquisition of a ^{13}C NMR; however, it was characterized by ^{1}H NMR, MS, IR, and UV−vis.

Even though the solubility of the compound is poor in organic solvents, it is sufficient to disperse SWCNTs because very dilute solutions are needed. SWCNTs cannot be dispersed in THF following method A (see Experimental Methods) even after extensive sonication. In constrast, SWCNTs were easily dispersed in THF solutions of **1** by sonication for a few minutes at room temperature, following exactly the same methodology. For characterization purposes, the excess of **1** was eliminated by centrifugation, and the resulting SWCNTs were dispersed in fresh THF. The resulting solutions were stable for days when maintained at 20−25 °C. In any case, if the tubes are subjected to temperature changes and precipitate, they could be easily redispersed by sonication for a few seconds.

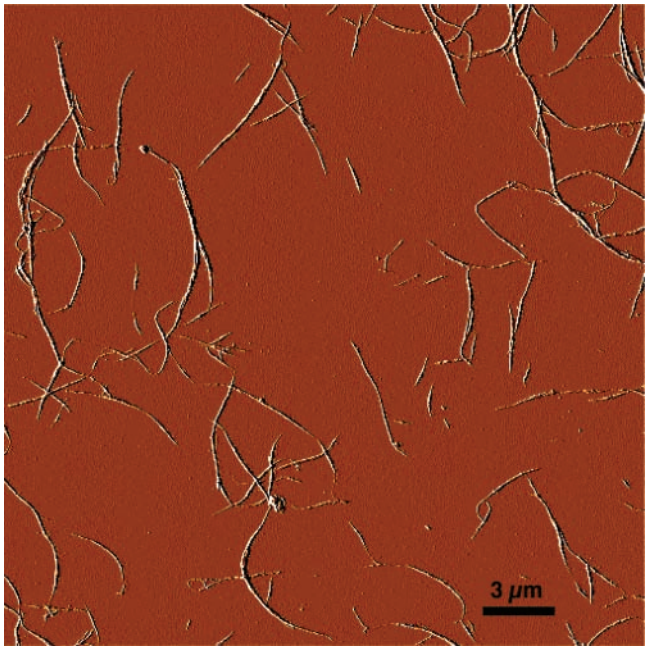

Figure 1. AFM images obtained by spin coating of a solution of SWCNT/**1**.

SCHEME 1: Synthesis and Preparation of Diazapentacene 1 and Its Assemblies with SWCNTs

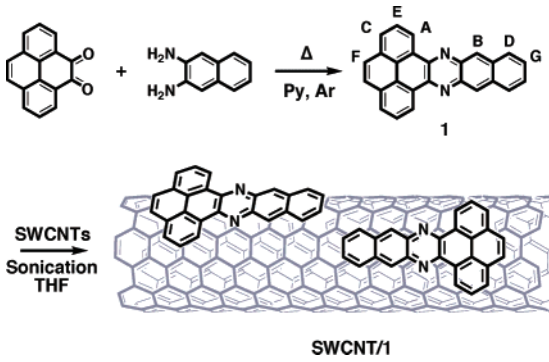

SWCNT/**1** dispersions were characterized by atomic force microscopy (AFM), which gave direct proofs of the presence of SWCNTs. The samples were deposited by spin coating from the THF solution. A representative image is shown in Figure 1, which shows bundles of tubes that appear all throughout the scanned area. The length of the bundles is in the order of several micrometers, while the diameters range from nanometer to micrometer.

UV−vis−NIR measurements of SWCNT/**1** dispersions show the van Hove singularities of metallic and semiconducting nanotubes in the vis−NIR region (Figure 2), while the signals corresponding to **1** were observed in the UV−vis region.

To identify the interactions that facilitate the dispersion of SWCNTs and to evaluate the degree of disturbance/disruption

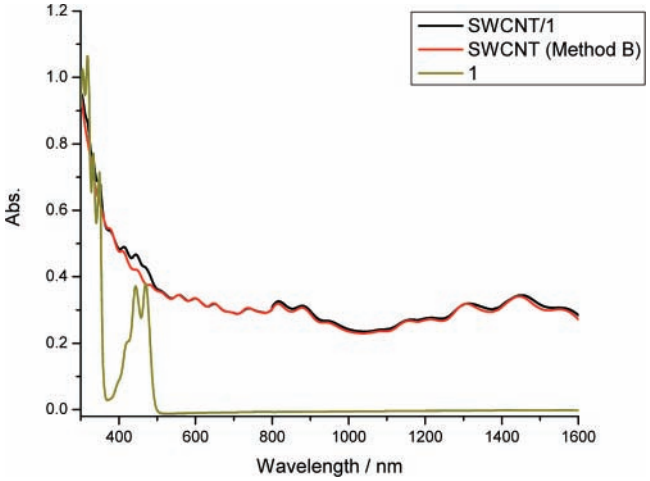

Figure 2. UV−vis−NIR of **1**, SWCNT, and SWCNT/**1** in THF.

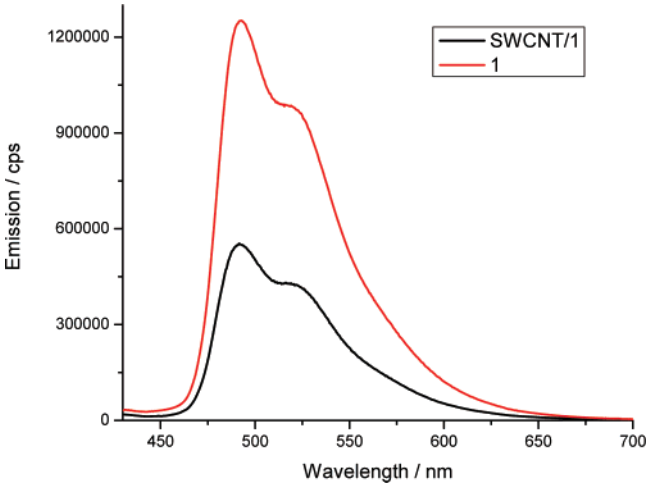

Figure 3. Room-temperature fluorescence spectra of **1** and SWCNT/**1** in THF with matching absorption at the 420 nm excitation wavelength.

of the properties of the SWCNTs effected by **1**, several photophysical measurements were carried out. The samples of SWCNT/**1** were prepared using method B (see Experimental Methods), because by this procedure it is possible to disperse SWCNTs in THF and also ensure that the SWCNTs are as much individually dispersed as possible. Through this tedious but more accurate method, SWCNTs were sonicated in THF in the presence of **1** at a fixed temperature of 20 °C, the excess of **1** was eliminated by centrifugation, and the nanotubes were resuspended by sonication at 20 °C. Conversely to method A, the SWCNT/**1** dispersions were prepared from dropwise dilution from the previous suspension followed by sonication. The UV−vis−NIR spectra of SWCNT/**1** prepared by method A or B present no differences, which is ideal for comparison purposes.

Interestingly, when comparing the overall dispersability of SWCNT and SWCNT/**1** in THF following method B, no appreciable differences were seen at first glance (Figure 2). Apparently, the absorption spectra of SWCNT/**1** suspensions are best described as the linear sum of SWCNT and **1**. For example, a superimposition of SWCNT and SWCNT/**1** reveals only differences in the region, where the **1** absorption is maximum at 305, 318, 333, 349, 443, and 470 nm. Moreover, subtracting the absorption spectrum of SWCNT from that of SWCNT/**1** brings just absorption of **1** to light. Important is that no broadening or shifts are noted. Nevertheless, small red shifts (in the order of 2 nm) evolve in the near-infrared region of the spectrum, which suggests the existence of weak interactions between SWCNTs and **1**.

To evaluate the excited-state interactions between SWCNTs and **1**, as a complement to the aforementioned ground-state interactions, we turned first to fluorescence spectroscopy (Figure 3). In particular, the strongly and long-lived fluorescent features of **1** were tested in the absence and presence of SWCNT. For **1**, we noticed a fluorescence peak with maxima at 493 nm and a shoulder around 520 nm. Considering the mirror image that such features imply, relative to the ground-state absorption, we assign these to the fundamental *0−0 transition. The quantum yield, determined with 1,10-diphenylanthracene as a standard, is 0.05 in THF. Additional features are seen in the 400−440 nm range, which are likely to originate from higher lying singlet excited states. While the fluorescence pattern for SWCNT/**1**, with matching absorption at the 420 nm excitation wavelength, is essentially identical to that seen for just **1**, its fluorescence intensity is decreased by about 58%. However, the overlapping absorption of SWCNT and **1** at the 420 nm excitation wavelength necessitates correction of the fluorescence intensity, because competing absorption of SWCNT and **1** leads to an inherent loss of **1** fluorescence. In doing so, it turns out that interactions between SWCNT and **1** do not show notable changes in the **1**-centered fluorescence. A similar conclusion is drawn from the time-resolved fluorescence measurements, where **1** and SWCNT/**1** were tested following 403 nm excitation. In particular, the major component of the 450 nm fluorescence maximum reveals a lifetime of 7.0 and 6.9 ns in the absence and presence of SWCNT, respectively.

Conclusive information about the nature of the interactions came from transient absorption spectroscopy (Figure 4). The excited-state properties of **1** and SWCNT are reference points for the interpretation of the features seen in SWCNT/**1**. The differential spectrum recorded immediately after a femtosecond 418 nm laser pulse for **1** is characterized by ground-state bleaching around 470 nm and broad absorptions between 550 and 750 nm as well as between 1000 and 1400 nm. These spectral attributes are indicative of the **1** singlet excited state and are formed with a rate constant of $\sim 1 \times 10^{12}$ s^{-1}. These features decay slowly on the picosecond time scale (5.5×10^{8} s^{-1}) to the energetically lower-lying triplet excited state via intersystem crossing. Features of the correspondingly formed triplet excited state are maxima 500 and 535 nm.

Looking at pristine SWCNTs, which were simply suspended in THF, a set of transient minima are seen to develop, upon 418 nm photoexcitation, at 1050, 1185, 1310, 1435, and 1555 nm. In the visible, additional minima are seen at 505, 555, 600, and 700 nm. Importantly, all of these features resemble the maxima seen in the ground-state absorption spectrum of a THF suspension of SWCNT. They all decay similarly to recover the ground state with two major components (i.e., 1.2 and 520 ps). We wish to emphasize that during the recovery of the ground state no particular shifts are observable.

Decisive are the experiments with SWCNT/**1**, exciting at 418 nm. The transient spectrum that develops early on (i.e., 0.8 ps after the laser pulse) is, surprisingly, dominated in the visible and in the near-infrared by features that correlate nicely with those seen for SWCNT. In particular, in the visible range (i.e., 400−800 nm), well-resolved minima appear at 505, 555, 600, and 700 nm that further extend in the near-infrared (i.e., 950−1650 nm) with minima at 1050, 1185, 1310, 1435, and 1555 nm. On the other hand, singlet excited-state characteristics of **1** that we had actually expected could not be detected at this stage. All of the aforementioned SWCNT fingerprints give rise in SWCNT/**1** to decay kinetics that are essentially identical to

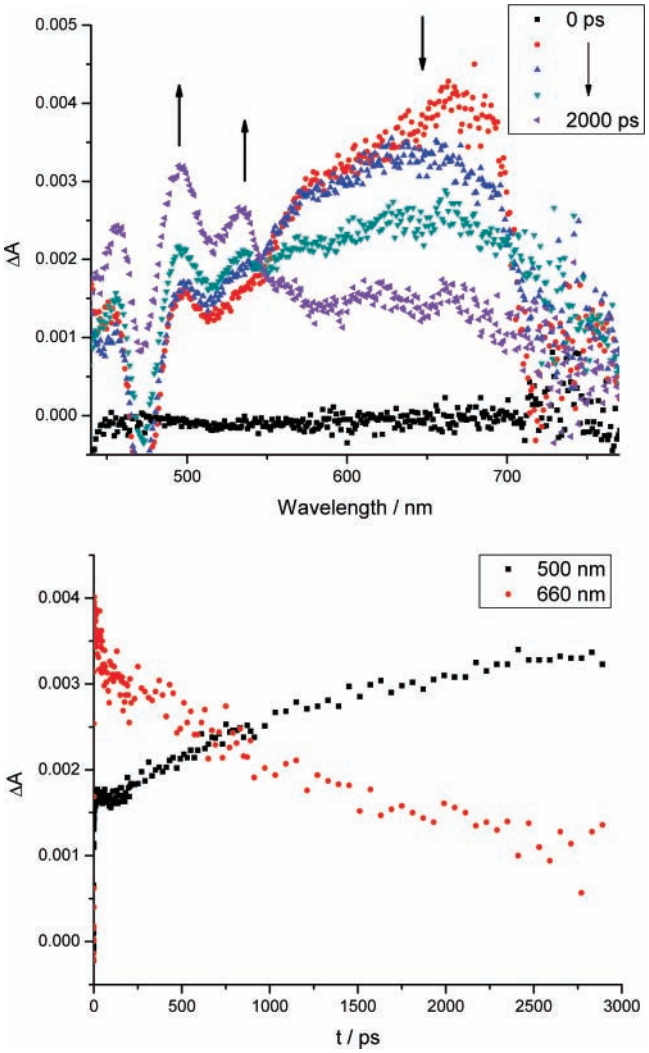

Figure 4. Differential absorption spectra (visible) obtained upon femtosecond flash photolysis (418 nm) of **1** in THF with several time delays between 2 and 2890 ps at room temperature (top) and the corresponding time profiles at 495 and 623 nm (bottom).

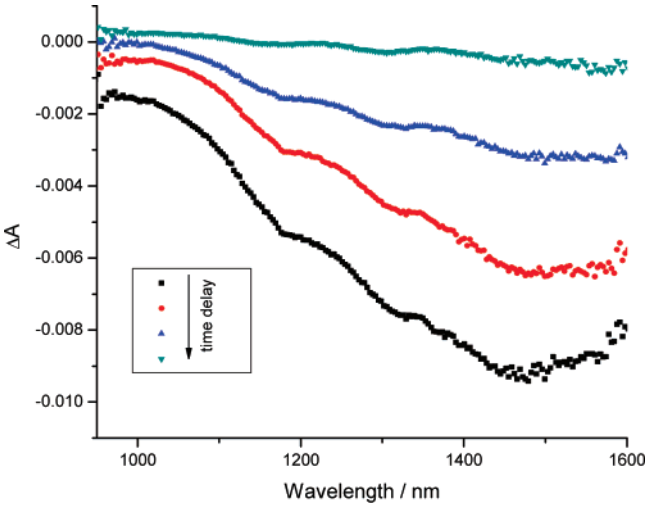

Figure 5. Differential absorption spectra (NIR) obtained upon femtosecond flash photolysis (418 nm) of SWCNT/**1** in THF with several time delays between 0.6 and 3.2 ps at room temperature.

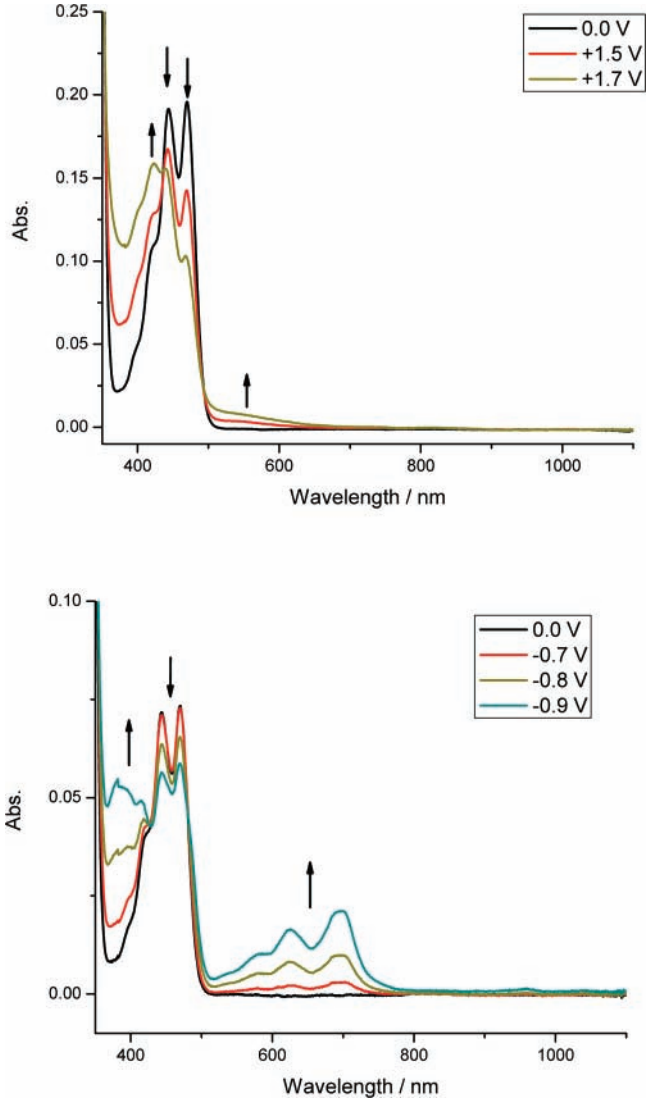

Figure 6. Spectroelectrochemistry of **1** in THF (0.2 M supporting electrolyte TBA PF_6) versus Ag wire under oxidative (top) and reductive (bottom) conditions.

that established for SWCNT (Figure 5). It is interesting to note that in the visible range (i.e., 505, 555, 600, and 700 nm) no notable shifts accompany the decay. Still, at a time delay of 5 ps or more a residual positive absorption remains, vide infra. Features in the near-infrared seem to shift slightly to the blue during the decay, but to a much lesser extent than what was reported recently.[31]

To shed light onto the nature/origin of the transient absorption that is seen in the visible range, we conducted spectroelectrochemistry with **1** in THF (Figure 6). In particular, we probed **1** under reductive and oxidative conditions. Under reductive conditions, new maxima evolve at 492, 622, and 698 nm, which we assign to the one-electron reduced species of **1**.[32,33] Contrary to the reduction, the following changes occur during the oxidation: new maximum at 422 nm. None of the changes that relate to the different redox state seem, however, to match the changes seen in the femtosecond experiments. This led us to consider a comparison with the **1** singlet excited-state features. In fact, a closer analysis reveals a fairly good spectroscopic agreement with the **1** singlet excited-state features, vide supra. Because the rapid decay of the SWCNT features and the formation of the **1** features do not relate, we must rule out any excited-state interactions between SWCNT and **1**.

Because we can rule out any solvophobic interactions from the chemical structure and the solvent used and also by taking into account that SWCNTs are easily dispersed in the presence

of **1**, we propose that solely $\pi-\pi$ interactions take place between SWCNTs and **1**. This agrees with the photophysical experimental data, where only small red shifts in the near-infrared region of the ground-state absorption and small blue shifts during the decay of the excited-state features have been observed, when comparing the absorption, emission, and transient absorption spectra of SWCNT/**1** with SWCNTs. This is also in agreement with previous work[9,11,12,21,22] where the $\pi-\pi$ interactions between the aromatic moiety and the surface of the nanotubes are strengthened by solvophobic interactions, because the aromatic systems are equipped with solvophilic groups that allow the dispersion of SWCNTs in aqueous solutions and force micellar interactions and organization. Therefore, by using simply weak $\pi-\pi$ interactions to disperse SWCNTs, their inherent properties are left virtually untouched.

Conclusions

We have presented how the dispersion of SWCNTs in THF can be easily achieved by sonication at room temperature in the presence of the novel diazapentacene **1**. The presence of SWCNTs in the dispersions was confirmed through AFM along with UV−vis−NIR, fluorescence, and transient absorption measurements. Photophysical experiments centered on **1** and on SWCNTs suggest that solely $\pi-\pi$ interactions are taking place between **1** and SWCNT. This is consistent with the fact that no solvophobic forces can participate in the interactions with the SWCNT walls, which is in agreement with the small changes observed in different ground-state and excited-state measurements. Therefore, we can conclude that **1** facilitates the dispersion of SWCNTs, without interfering with their electronic properties, which makes this approach very appealing for the manipulation of SWCNTs for electronic applications.

Acknowledgment. This work was carried out with partial support from the University of Trieste, INSTM, MUR (PRIN 2006, prot. 2006034372 and FIRB, prot. RBNE033KMA), the Deutsche Forschungsgemeinschaft (SFB 583), FCI, and the Office of Basic Energy Sciences of the U.S. Department of Energy (NDRL 4717). We thank the Vigoni program for a travel grant between Trieste and Erlangen. K.H.C. acknowledges a grant from DAAD (RISE scholarship program). We are grateful to Dr. Fabio Hollan for the mass spectrometry measurements.

References and Notes

(1) Anthony, J. E. *Chem. Rev.* **2006**, *106*, 5028.
(2) Wu, Z.; Chen, Z.; Du, X.; Logan, J. M.; Sippel, J.; Nikolou, M.; Kamaras, K.; Reynolds, J. R.; Tanner, D. B.; Hebard, A. F.; Rinzler, A. G. *Science* **2004**, *305*, 1273.
(3) Gruner, G. *J. Mater. Chem.* **2006**, *16*, 3533.
(4) Forrest, S. R. *Nature* **2004**, *428*, 911.
(5) Tasis, D.; Tagmatarchis, N.; Bianco, A.; Prato, M. *Chem. Rev.* **2006**, *106*, 1105.
(6) Zhang, J.; Lee, J. K.; Wu, Y.; Murray, R. W. *Nano Lett.* **2003**, *3*, 403.
(7) Gregan, E.; Keogh, S. M.; Maguire, A.; Hedderman, T. G.; Neill, L. O.; Chambers, G.; Byrne, H. J. *Carbon* **2004**, *42*, 1031.
(8) Hedderman, T. G.; Keogh, S. M.; Chambers, G.; Byrne, H. J. *J. Phys. Chem. B* **2004**, *108*, 18860.
(9) Sandanayaka, A. S. D.; Takaguchi, Y.; Uchida, T.; Sako, Y.; Morimoto, Y.; Araki, Y.; Ito, O. *Chem. Lett.* **2006**, *35*, 1188.
(10) Hedderman, T. G.; Keogh, S. M.; Chambers, G.; Byrne, H. J. *J. Phys. Chem. B* **2006**, *110*, 3895.
(11) Takaguchi, Y.; Tamura, M.; Sako, Y.; Yanagimoto, Y.; Tsuboi, S.; Uchida, T.; Shimamura, K.; Kimura, S.; Wakahara, T.; Maeda, Y.; Akasaka, T. *Chem. Lett.* **2005**, *34*, 1608.
(12) Tomonari, Y.; Murakami, H.; Nakashima, N. *Chem.-Eur. J.* **2006**, *12*, 4027.
(13) Gotovac, S.; Honda, H.; Hattori, Y.; Takahashi, K.; Kanoh, H.; Kaneko, K. *Nano Lett.* **2007**, *7*, 583.
(14) Chen, R. J.; Zhang, Y. G.; Wang, D. W.; Dai, H. J. *J. Am. Chem. Soc.* **2001**, *123*, 3838.
(15) Liu, L.; Wang, T. X.; Li, J. X.; Guo, Z. X.; Dai, L. M.; Zhang, D. Q.; Zhu, D. B. *Chem. Phys. Lett.* **2003**, *367*, 747.
(16) Petrov, P.; Stassin, F.; Pagnoulle, C.; Jerome, R. *Chem. Commun.* **2003**, 2904.
(17) Gomez, F. J.; Chen, R. J.; Wang, D. W.; Waymouth, R. M.; Dai, H. J. *Chem. Commun.* **2003**, 190.
(18) Fernando, K. A. S.; Lin, Y.; Wang, W.; Kumar, S.; Zhou, B.; Xie, S. Y.; Cureton, L. T.; Sun, Y. P. *J. Am. Chem. Soc.* **2004**, *126*, 10234.
(19) Artyukhin, A. B.; Bakajin, O.; Stroeve, P.; Noy, A. *Langmuir* **2004**, *20*, 1442.
(20) Georgakilas, V.; Tzitzios, V.; Gournis, D.; Petridis, D. *Chem. Mater.* **2005**, *17*, 1613.
(21) Guldi, D. M.; Rahman, G. M. A.; Jux, N.; Balbinot, D.; Hartnagel, U.; Tagmatarchis, N.; Prato, M. *J. Am. Chem. Soc.* **2005**, *127*, 9830.
(22) Ehli, C.; Rahman, G. M. A.; Jux, N.; Balbinot, D.; Guldi, D. M.; Paolucci, F.; Marcaccio, M.; Paolucci, D.; Melle-Franco, M.; Zerbetto, F.; Campidelli, S.; Prato, M. *J. Am. Chem. Soc.* **2006**, *128*, 11222.
(23) Guldi, D. M.; Menna, E.; Maggini, M.; Marcaccio, M.; Paolucci, D.; Paolucci, F.; Campidelli, S.; Prato, M.; Rahman, G. M. A.; Schergna, S. *Chem.-Eur. J.* **2006**, *12*, 3975.
(24) Nakashima, N. *Sci. Tech. Adv. Mater.* **2006**, *7*, 609.
(25) Toyoda, S.; Yamaguchi, Y.; Hiwatashi, M.; Tomonari, Y.; Murakami, H.; Nakashima, N. *Chem. Asian J.* **2007**, *2*, 145.
(26) Holder, P. G.; Francis, M. B. *Angew. Chem., Int. Ed.* **2007**, *46*, 4370.
(27) Curran, S. A.; Ajayan, P. M.; Blau, W. J.; Carroll, D. L.; Coleman, J. N.; Dalton, A. B.; Davey, A. P.; Drury, A.; McCarthy, B.; Maier, S.; Strevens, A. *Adv. Mater.* **1998**, *10*, 1091.
(28) Woo, H. S.; Czerw, R.; Webster, S.; Carroll, D. L.; Ballato, J.; Strevens, A. E.; O'Brien, D.; Blau, W. J. *Appl. Phys. Lett.* **2000**, *77*, 1393.
(29) Star, A.; Stoddart, J. F.; Steuerman, D.; Diehl, M.; Boukai, A.; Wong, E. W.; Yang, X.; Chung, S. W.; Choi, H.; Heath, J. R. *Angew. Chem., Int. Ed.* **2001**, *40*, 1721.
(30) Hu, J.; Zhang, D.; Harris, F. W. *J. Org. Chem.* **2005**, *70*, 707.
(31) Ballesteros, B.; Campidelli, S.; de la Torre, G.; Ehli, C.; Guldi, D. M.; Prato, M.; Torres, T. *Chem. Commun.* **2007**, *28*, 2950.
(32) Alonso, A. M.; Horcajada, R.; Groombridge, H. J.; Mandalia, R.; Motevalli, M.; Utley, J. H. P.; Wyatt, P. B. *Chem. Commun.* **2004**, *10*, 412.
(33) Alonso, A. M.; Horcajada, R.; Motevalli, M.; Utley, J. H. P.; Wyatt, P. B. *Org. Biomol. Chem.* **2005**, *3*, 2842.